BBA - Molecular Cell Research 1866 (2019) 118555

Contents lists available at ScienceDirect

BBA - Molecular Cell Research

journal homepage: www.elsevier.com/locate/bbamcr

A switch of N-glycosylation of proteome and secretome during differentiation of intestinal epithelial cells

Paweł Link-Lenczowski[a,*], Martyna Jastrzębska[a], Katarzyna Chwalenia[a,c], Małgorzata Pierzchalska[b], Anna Leja-Szpak[a], Joanna Bonior[a], Piotr Pierzchalski[a,1], Jolanta Jaworek[a,1]

[a] Department of Medical Physiology, Faculty of Health Sciences, Jagiellonian University Medical College, Kraków, Poland
[b] Department of Food Biotechnology, Faculty of Food Technology, The University of Agriculture in Kraków, Kraków, Poland
[c] Department of Paediatrics, University of Oxford, Oxford, United Kingdom

ARTICLE INFO

Keywords:
Colon adenocarcinoma
Enterocyte
Glycosylation
Glycome
Secretome
Differentiation

ABSTRACT

The maintenance of homeostasis of the intestinal epithelium depends on the complex process of epithelial cells differentiation, which repeatedly continues throughout the entire life. Many studies suggest, that cellular differentiation is regulated by glycosylation, or at least that changes of the latter are the hallmark of the process. The detailed description and understanding of this relationship are important in the context of gastrointestinal tract disease, including cancer. Here we employ a broadly used *in vitro* model of intestinal cell differentiation to track the glycosylation changes in details. We analyzed the *glycoproteome*- and *glycosecretome*-derived N-glycomes of undifferentiated Caco-2 adenocarcinoma cells and Caco-2-derived enterocyte-like cells. We used HILIC-HPLC and MALDI-ToF-MS approach together with exoglycosidases digestions to describe qualitative and quantitative N-glycosylation changes upon differentiation. Derived glycan traits analysis revealed, that differentiation results in substantial upregulation of sialylation of *glycoproteome* and increment of fucosylation within *glycosecretome*. This was also clearly visible when we analyzed the abundances of individual glycan species. Moreover, we observed the characteristic shift within oligomannose N-glycans, suggesting the augmentation of mannose trimming, resulting in downregulation of H8N2 and upregulation of H5N2 glycan. This was supported by elevated expression of Golgi alpha-mannosidases (especially MAN1C1). We hypothesize, that intensified mannose trimming at the initial steps of N-glycosylation pathway during differentiation, together with the remodeling of the expression of key glycosyltransferases leads to increased diversity of N-glycans and enhanced fucosylation and sialylation of complex structures. Finally, we propose H4N5F1 glycan as a potential biomarker of intestinal epithelial cell differentiation.

1. Introduction

Protein glycosylation is the universal feature of all eukaryotic cells. It is also the most frequent post-translational modification, which introduces the enormous potential of biodiversity, strongly exceeding the one resulted from the informational capacity of the genomes themselves [1]. The function of glycans reveals at the protein level, where they guarantee proper folding, modify polarity or protect against proteolysis [2]. Moreover, it is well known that glycosylation modifies or regulates a broad variety of physiological mechanisms including morphogenesis, cell growth and differentiation, cell proliferation, apoptosis as well as intrinsic and extrinsic cellular interactions [3]. Therefore, it is not surprising that the ever-growing number of evidence underline the importance of glycans in human diseases, including cancer [4]. The N-glycosylation of proteins is a multistep process taking place along the secretory pathway, involving initial trimming of oligomannose precursor oligosaccharide and its further modifications by Golgi glycosyltransferases to form hybrid and complex N-glycans. Although the

Abbreviations: 2-AB, 2-aminobenzamide; AA, 2-aminobenzoic acid; F, fucose; H, hexose; HILIC, hydrophilic interaction liquid chromatography; MET, Mesenchymal-Epithelial-Transition; ManNAz, *N*-azidoacetylmannosamine; N, *N*-acetylhexosamine; S, *N*-acetylneuraminic acid

* Corresponding author at: Department of Medical Physiology, Faculty of Health Sciences, Jagiellonian University Medical College, Michałowskiego 12, 31-126 Kraków, Poland.
E-mail address: p.link-lenczowski@uj.edu.pl (P. Link-Lenczowski).
[1] These authors share senior authorship.

https://doi.org/10.1016/j.bbamcr.2019.118555
Received 15 April 2019; Received in revised form 27 August 2019; Accepted 4 September 2019
Available online 06 September 2019
0167-4889/

glycosylation machinery has been well described [5], the details of the regulation of the process and the mechanisms leading to the formation of a specific type of sugar repertoire on the cellular *glycoproteome* remain the subject of intensive research.

The intestinal epithelium is a multifunctional barrier that is responsible not only for digestive functions of the organism but also interacts with commensal microbiota and serves as a first line of defense against pathogens. The small intestine epithelium is divided into crypts and villi, that project into the intestinal lumen. Under physiological conditions, the crypt-based proliferative stem cells give rise to all five cell types: enterocytes, goblet cells, enteroendocrine cells, Paneth cells, and Tuft cells [6]. The differentiated cells reaching the top of a villus undergo apoptosis by anoikis and are shed into the intestinal lumen every 3–5 days [7]. The dynamics and the high rate of cellular turnover suggest complex regulation of cell proliferation, differentiation and death and disruption of these processes is considered as one of the causes of intestinal diseases, including cancer [8]. The most numerous cell type within the intestinal epithelium is enterocytes which undergo dramatic morphological and physiological changes during differentiation. As their main function is the final digestion, efficient absorption and transport of nutrients from the intestinal lumen into the blood stream, the mature enterocytes are polarised, forming microvilli which enlarge the luminal surface and are the place of the anchorage of brush border hydrolases. Up to date, the precise mechanisms regulating intestinal epithelial cells differentiation are still not entirely known. As the regulation of proliferation and differentiation within the intestinal epithelium is very complex, it is realized at many different levels. Besides classical signaling such as Wnt, Notch and PI3K/Akt/mTOR pathways, which are the basics of the regulation of intestinal homeostasis other mechanisms are postulated, such as epigenetic changes and metabolic states of the cells [9–13]. Protein glycosylation is known to play an important role in mammalian development, starting from fertilization of the oocyte and perturbations in glycosylation machinery strongly impairs organogenesis or are even lethal [14–16]. Currently, the major emphasis is being placed on looking for specific glyco-markers of differentiation steps. Unfortunately, the studies concerning a description of regulatory mechanisms responsible for glycosylation changes during cellular differentiation are very limited. It seems that lineage-specific glycosylation is crucial for gaining the proper mature cell phenotype. These changes will influence not only the function of individual glycoproteins, which expression is regulated during differentiation but also will be important for membrane organization, interaction with other cells and their surrounding and modulation of "outside-in" and "inside-out" cellular signals. There are still growing number of evidence presenting changes within the N-glycomes of differentiating cells, suggesting the occurrence of specific shifts within glycosylation pathway during differentiation [17–19]. Some of these glycan changes (e.g. α2-6 sialylation) are also suggested as marker of the differentiation potential of stem cells [20]. The majority of these reports discuss carbohydrate antigens mainly in the context of embryonic, mesenchymal and neural stem cells differentiation. Although the luminal surface of the intestinal epithelium is heavily glycosylated [21], the importance of glycosylation changes and their regulation during intestinal epithelial cells differentiation has not been studied very deeply. Some data suggest that the evolution of oligomannose chains to complex chains could be a characteristic feature of microvillus membrane during intestine development [22]. Unfortunately, the *in vitro* studies of intestinal epithelial cell differentiation are strongly limited. The Caco-2 human adenocarcinoma cell line is broadly used as an *in vitro* model of absorptive intestinal epithelial cells, due to its unique ability to spontaneous differentiation into enterocyte-like cells upon long-term culture conditions. Several days after reaching the confluence Caco-2 cells form an integral monolayer of polarised cells with functional microvilli at the apical surface and when differentiated they also exhibit strong expression of brush border hydrolases [23]. The membrane polarization of enterocyte is partially possible due to specific protein sorting within the cells. Recent years have shown, that N-glycosylation of proteins can be crucial in this process. For example, apical sorting of membrane dipeptidases in Caco-2 cells is dependent on N-glycosylation [24]. The role of specific oligosaccharide structures in this process is poorly understood. It has been published, however, that sialylation of glycans can be an important mediator in apical delivery [25].

In the case of Caco-2-based cellular model, we still do not have a complete picture of modulations in glycan synthesis during differentiation towards enterocyte-like phenotype. The early studies based on plant lectin microarrays and lectin blotting showed a decrease in reactivity of glycoproteins with sialic acid binding agglutinins (SNA and MAA) and fucose-binding UEA lectin during differentiation [26]. Other data also suggest some important changes in sialic acid distribution in differentiated enterocytes as well as down-regulation of fucosylation [27,28]. Finally, the specific modulation of glycosyltransferases activity during Caco-2 cells differentiation was described, showing up-regulation of several GlcNAc transferases during this process, but without further continuation with glycomic studies [29]. The detailed understanding of glycosylation changes during maturation of intestinal epithelium appears crucial to learn the exact causes and biology of gastrointestinal tract diseases, including cancer. The transformation and progression of many malignancies are associated with glycosylation changes and some glycan epitopes are considered as cancer biomarkers [30–32]. Malignant transformation of gastrointestinal tract tissue is one of the most important medical problems nowadays, and a number of studies concerning the importance of glycosylation in biology and pathology of these diseases is still growing. Previously published data clearly show that colorectal cancer tissue is characterized by the higher content of paucimannosidic glycans, sialylated Lewis type epitopes and sulfated structures, whereas bisecting GlcNAc expression is down-regulated in tumor tissue [33]. Moreover, the analyses of patient's sera indicate the alterations within N-glycomes towards the increased size of complex structures (diantennary *vs*. multiantennary) and sialylation in colorectal cancer, proving a strong prognostic value of these changes [34]. In this context, the studies on glycosylation changes accompanying the differentiation process within intestinal epithelia may bring us closer to understanding their biological importance in GI malignancies. As Caco-2 cells have the ability to differentiate *in vitro* they can be treated as a useful model for tracking the process of losing the malignant phenotype (adenocarcinoma) by cancer cells. This is interesting, partially in context of cancer stem cells theory and so-called epithelial-to-mesenchymal and mesenchymal-to-epithelial transition, but also in the context of cancer differentiation therapy [35,36].

Recently, Park et al. employing nano-LC/ESI QTOF mass spectrometry have presented a detailed study on qualitative and quantitative glycosylation changes of plasma membrane-associated glycoproteins during Caco-2 cells differentiation [37]. They showed a decrease in oligomannose type glycans and upregulation of sialylation and fucosylation of complex and hybrid structures during differentiation, together with a qualitative comparison of abundance of the individual glycan species. Here, using HILIC-HPLC and MALDI-ToF-MS we are describing the N-glycomic studies of total cellular *glycoproteome* and *glycosecretome* to complete the picture of glycosylation changes of differentiating Caco-2 cells. We also aimed to present a quantitative comparison of selected glycosylation-related genes expression during differentiation.

2. Materials and methods

2.1. Reagents

2-aminobenzamide (2-AB), 2-mercaptoethanol, acrylamide, anthranilic acid (AA), ammonium persulfate (APS), bisacrylamide, bovine serum albumin (BSA), dimethyl sulfoxide (DMSO), Dulbecco's phosphate-buffered saline (DPBS), ethidium bromide, glycine, sodium

dodecyl sulfate (SDS), sodium cyanoborohydride, TEMED, trifluoroacetic acid (TFA) and Trizma® Base were purchased from Sigma-Aldrich (Poznań, Poland). PageRuler Prestained Protein Ladder and Laemmli Sample Buffer were obtained from Fermentas (Thermo Fisher Scientific, Warszawa, Poland). Fetal Bovine Serum (FBS) was purchased from Eurx (Gdańsk, Poland). 2,5-dihydroxybenzoic acid (2,5-DHB) was from Bruker Daltonics (Bremen, Germany). Acetonitrile HPLC grade for far UV J.T. Baker was from Avantor (Gliwice, Poland). All other salts, alcohols and acids were of analytical grade and were provided by Sigma-Aldrich.

2.2. Cells and culture conditions

Caco-2 cells (ATCC® HTB-37™) were grown in Dulbecco's Modified Eagle Medium (DMEM) supplemented with 4 mM L-glutamine, 25 mM glucose, 10% FBS, Non-essential Amino Acids, 0,25 mg/L amphotericin B, 100 U/L penicillin and 100 mg/L streptomycin (Biowest, Nuaillé, France). Cells were grown with 5% CO_2 at 37 °C and were passaged at 70–80% confluency. For each experiment cells from the same passage were used and were analyzed in biological triplicates at three time points: sub-confluent cells, 4 days after reaching the confluence and 12 days post-confluence. Cultures were systematically tested by PCR for the presence of *Mycoplasma sp*.

2.3. Immunofluorescence microscopy

Cells were grown on round glass coverslips (13 mm) in a 12-well plate under conditions described above. The cells were washed 3 times with DPBS, fixed with 3.7% phosphate-buffered formaldehyde at room temperature for 20 min and washed 3 times with DPBS. Unspecific protein binding was blocked with Universal Blocker™ blocking buffer (Thermo Fisher Scientific) for 1 h and the specimens were incubated overnight at 4 °C with primary antibodies diluted in Universal Blocker (1:500; Anti-Sucrase-Isomaltase antibody produced in rabbit, polyclonal SAB2102141, Sigma-Aldrich). The coverslips were washed in TBS (3 × 10 min with gentle agitation) and incubated with anti-rabbit Alexa Fluor®488 conjugated antibodies (1:1000, Cell Signaling Technology, USA) for 1 h at RT. After washing, the cells were counterstained with Hoechst 33342 (Molecular Probes, 1 μg/ml) and washed three times with PBS. The cells were observed under AxioObserver Z.1 microscope controlled by Zen 2012 software (Zeiss, Oberkochen, Germany) and the images were taken by AxioCam HR digital camera.

2.4. Scanning electron microscopy (SEM)

Cells were grown on glass coverslips in a 12-well plate under standard conditions. At three time points (sub-confluency, 4 and 12 days post-confluency), the cells were washed 3 times with DPBS and then fixed with 2.5% of glutaraldehyde phosphate buffered saline solution for 1 h at RT. Fixed cells were washed three times with DPBS, dehydrated in a series of water-ethanol solutions (15%–70%) and dried by the critical point procedure (E3000 Critical point dryer, Quorum Technologies, Laughton, UK). Finally, the specimens were gold-coated in JFC-1100 ion sputter (Jeol, Warszawa, Poland) and scanning micrographs were taken on JEOL JSM5410 electron microscope.

2.5. Alkaline phosphatase activity assay

Alkaline phosphatase activity was measured in cell lysates using a colorimetric assay with *p*-nitrophenyl phosphate (*p*-NPP) as a substrate. Briefly, 30 μg of homogenate proteins were diluted with assay buffer (0.1 M sodium carbonate-bicarbonate pH 9.5, 5 mM $MgCl_2$, 7 mM *p*-NPP) up to 150 μL in a 96-well plate and incubated at 37 °C in the EL808 microplate reader (BioTek, Winooski, VT). At every 10 min of the incubation, the absorbance at 405 nm was read to measure the concentration of produced yellow *p*-nitrophenyl (*p*-NP). Along with the samples, a standard curve of *p*-NP (5–120 nmol) was prepared. The specific enzymatic activity was calculated from the linear range of product production and was expressed as mU/mg of protein (1 mU = 1 nmol of *p*-NP/min, at 37 °C).

2.6. Cell lysis and isolation of secreted proteins

One day before each time point the cells were washed 5 times with DPBS and then cultured in culture medium without FBS. After 24 h, the culture media containing secreted proteins were collected, filtered through a 0.2 μm pore size filter and frozen at −80 °C. The cells were washed 3 times with DPBS, harvested with a rubber scraper in cold DPBS and centrifuged at 500 xg for 5 min at 4 °C. The cells were lysed by pipetting in lysis buffer (50 mM Tris-HCl, pH 8.0, 150 mM NaCl, 0,5% Triton-X-100, proteinases inhibitor cocktail) and the protein extracts were cleared by centrifugation at 4 °C and kept at −80 °C for storage. Protein concentration was measured by BCA method according to manufacturer's protocol (Micro BCA™ Protein Assay Kit, Thermo Fisher Scientific, Warszawa, Poland).

2.7. SDS-PAGE and Western blotting

Cell lysate proteins (15 μg) were resuspended in Laemmli sample buffer, denatured by boiling (100 °C, 5 min) and separated on 8% polyacrylamide gels, according to Laemmli [38]. Molecular masses of proteins were determined using a prestained protein standard. Separated proteins were transferred onto an Immobilon-P PVDF membrane (Bio-Rad, Warszawa, Poland) according to the method described by Towbin et al. [39]. The membranes were blocked with 1% BSA in TBST (50 mM Tris pH 7.5, 150 mM NaCl, 0.1% Tween 20) for 60 min and then incubated with antibodies (Santa Cruz Biotechnology, Heidelberg, Germany) against SI (1:400), ALPI (1:1000) or beta-actin (1:400) for 60 min with constant shaking. After that, membranes were washed in TBST (3 × 15 min), incubated with secondary antibodies conjugated with horseradish peroxidase (1:7500) for 1 h and finally washed three times with TBST. To detect chemiluminescent protein bands, the membranes were incubated with SuperSignal® West Pico Chemiluminescent Substrate (Thermo Fisher Scientific, Warszawa, Poland) for 5 min and visualized on X-ray film.

2.8. Reverse transcription quantitative PCR (qPCR)

Total RNA was isolated from cells using GeneMATRIX Universal RNA/miRNA Purification Kit (EurX, Gdańsk, Poland) according to the manufacturer's protocol. For the first strand cDNA synthesis NG dART RT kit (EurX) was used with oligo(dT) as a primer and 1 μg of total RNA as a template. For qPCR 1 μL template cDNA, 0.5 μM of each primer (for primers list see Supplementary Table 1). and SG qPCR Master Mix (EurX) were used in a total volume of 10 μL. The amplification was carried out in CFX96 Touch™ Real-Time PCR Detection System (Bio-Rad) under following conditions: initial denaturation at 95 °C for 10 min, 35 cycles of 15 s at 94 °C, 30 s at 60 °C and 30 s at 72 °C. *GAPDH* was used as a reference gene for normalization and each gene expression was presented as relative to undifferentiated cells. GenEx 6.1 trial version software (Multid Analyses AB, Göteborg, Sweden) was used for data processing.

2.9. Glycoproteins deglycosylation and glycan labeling

Before deglycosylation, the secreted (*glycosecretome*) and cell lysate (*glycoproteome*) proteins were concentrated by chemical precipitation as described previously [40]. Dried protein pellets were resuspended in 20 μL of reducing buffer (0.5% SDS, 1% 2-mercaptoethanol), denatured at 100 °C for 10 min and after cooling to RT, 4 μL of 10% NP-40 was added. After that, 4 μL of 0.5 M sodium phosphate buffer, pH 7.5 was added followed by 1 μL of PNGase F (500,000 U/ml, New England

Biolabs, Ipswich, MA). The glycoproteins were deglycosylated in a total volume of 40 µL at 37 °C overnight. The released N-glycans were desalted by solid phase extraction (SPE) on Supelclean™ ENVI-Carb™ SPE columns (Sigma-Aldrich) according to Packer et al. [41] and eluted glycans were dried-down on SpeedVac. Next, the released oligosaccharides were labeled with anthranilic acid (AA) according to Anumula and Dhume [42] modified by Neville et al. [43] for MS analysis or with 2-aminobenzamide (2-AB) according to Bigge et al. [44] for HPLC analysis. Fluorescently labeled N-glycans were purified on *Spe-ed* Amide-2 SPE columns (Pelican Scientific, Tattenhall, U.K.) as previously described [40].

2.10. HILIC-HPLC analysis of fluorescently labeled N-glycans

Purified 2-AB-oligosaccharides were separated by HILIC-HPLC using a 4.6 × 150 mm TSK gel-Amide 80 column (3 µm bead size) (Tosoh Bioscience, Griesheim, Germany) on Shimadzu Prominence HPLC system (Shimadzu, Duisburg, Germany) with an in-line RF-20Axs fluorescence detector set at Exλ 330 nm and Emλ 420 nm. Solvent A was acetonitrile (ACN). Solvent B was 50 mM ammonium hydroxide, titrated to pH 4.4 with formic acid, in Milli-Q water. Samples were loaded in 70% ACN and all chromatography was performed at 50 °C using high-resolution gradient conditions at a flow rate of 1.25 mL/min: time = 0 min (t = 0), 30% B; t = 30.25, 48% B; t = 31, 100% B; t = 33, 100% B; t = 34, 30% B; t = 40, 30% B. Chromatography was controlled, and data were collected using Shimadzu LabSolutions 5.90 software. Each set of 10 runs was externally standardized with a 2AB-labeled glucose oligomer ladder external standard (Glyko Prozyme, Hayward, CA). The glucose units (GU) for each peak were calculated in GraphPad Prism trial version (GraphPad Software, La Jolla, CA). Basing on the GU values, the initial annotation of glycan peaks was performed based on GlycoStore database (www.glycostore.org) [45,46].

2.11. Exoglycosidase digestion of 2-AB-labeled N-glycans

To confirm the structures of the *N*-glycans, exoglycosidase digestions were performed. The 2-AB-labeled glycan aliquots were dried-down on speed-vac, resuspended in 50 mM sodium acetate pH 5.5, 5 mM $CaCl_2$ buffer and digested sequentially with *Arthrobacter ureafaciens* sialidase (ABS; EC 3.2.1.18, 0.5 U/mL), bovine testes β(1-3,4)-galactosidase (BTG; EC 3.2.1.23, 0.5 U/mL), bovine kidney α(1-2,3,4,6)-fucosidase (BKF; EC 3.2.1.51, 0.5 U/mL), jack bean β-*N*-acetylhexosaminidase (JBH; EC 3.2.1.52, 5 U/mL) and jack bean α(1-2,3,6)-mannosidase (JBM; EC 3.2.1.24, 15 U/mL). Enzymes were supplied by Glyko® (ProZyme, Ballerup, Denmark) and all reactions were carried out overnight at 37 °C. Following digestion, samples were purified with cotton microtips according to Selman et al. [47] and analyzed by HILICPLC-HPLC as described above.

2.12. MALDI-ToF-MS

Dried AA labeled glycans were reconstituted in 10 µL of 0.1% TFA in water and desalted with C18ZipTipTM (Millipore, Merck, Warszawa, Poland) following the manufacturer's instructions. Glycans were eluted with a 2,5-dihydroxybenzoic acid solution (10 mg/mL in 50/50, ACN/water containing 0.1% TFA) directly onto a MALDI target plate and dried at RT.

MALDI-ToF-MS was performed on UltrafleXtreme™ mass spectrometer controlled by FlexControl software (Bruker Daltonics, Bremen, Germany). The instrument was externally calibrated using the Bruker peptides calibration kit (757.4 Da – 3147.5 Da). The mass spectra were acquired in the negative ion reflectron mode over the m/z range from 700 to 5000 for a total of 5000 shots/sample. Glycan peaks were annotated basing on the m/z values and common knowledge of glycobiology using GlycoWorkbench (Version 1.1, European Carbohydrates DataBase project; http://www.eurocarbdb.org/). GlycoWorkbench was also used for preparing graphical representations of N-glycans.

2.13. Metabolic labeling and detection of sialo-proteome with N-azidoacetylmannosamine (ManNAz) and "click" chemistry

The cells were cultured with or without the presence of 50 µM Ac_4ManNAz (Thermo Fisher Scientific). ManNAz is metabolically converted to the corresponding azido sialic acid (SiaNAz) and incorporated into cellular glycans. At each time point (see 2.2) the cells were washed with cold DPBS, harvested and lysed as described above (see 2.6). Fifty µg of cell lysate proteins were chemically precipitated as described above (see 2.9) and the protein pellets were resuspended in solubilization buffer (50 mM Tris-HCl pH 8.0, 1% SDS) to obtain the protein concentration of 2 mg/mL. The azido sugar modified glycoproteins were labeled with alkyne-biotin (Thermo Fisher Scientific) using Click-iT™ Protein Reaction Buffer Kit (Thermo Fisher Scientific) according to the manufacturer's instructions. Biotinylated glycoproteins were separated on 10% polyacrylamide gel and transferred onto PVDF membrane as described above (see 2.7). The membranes were blocked in 1% BSA in TBST for 1 h at RT, washed 3 times in TBST and incubated with streptavidin-HRP conjugate (1:40000, Sigma-Aldrich) for 60 min After washing three times with TBST the membranes were incubated with SuperSignal® West Pico Chemiluminescent Substrate (Thermo Fisher Scientific, Warszawa, Poland) for 5 min and biotinylated protein bands were visualized on X-ray film. Finally, PVDF membranes were stained with Coomassie Brillant Blue (CBB) and the optical density of protein lanes form X-ray films and PVDF membranes were measured using ImageJ software. To compare the sialylation status of the samples, the optical density of the whole lanes was normalized to the corresponding CBB staining. The specificity of the sialic acid staining was verified with the use of *Arthrobacter ureafaciens* sialidase (data not shown).

2.14. Data processing and statistical methods

For glycan analysis, abundances of individual glycan species were normalized to the sum of peak areas of all glycans detected using Bruker's FlexControl software (MALDI-MS), and were presented as percentages of total glycans abundance. Additionally, glycans were grouped into 9 derived glycan traits, reflecting main glycan-types (paucimannosidic, oligomannose, hybrid, and complex glycans), their complexity (diantennary, triantennary and multiantennary glycans) and common structural characteristics (sialylated and fucosylated glycans). The abundance of each glycan trait was calculated as a sum of the relative intensities of the selected individual glycans (Supplementary Table 3). For qPCR, an initial data processing was done using GenEx 6.1 trial version software (Multid Analyses AB, Göteborg, Sweden). The Grubbs' test was performed for detecting potential outliers, and the data were normalized to the reference gene (glyceraldehyde-3-phosphate dehydrogenase, *GAPDH*) and presented as relative to undifferentiated cells in log2 scale. In all cases, data are presented as means ± standard deviation (SD). To determine statistical significance between the average values of 3 biological replicates, a two-tailed unpaired t-test was performed using GraphPad Prism trial version (GraphPad Software).

2.15. Key resources table

Resource	Source	Identifier
Antibodies		
Anti-rabbit Alexa Fluor®488 conjugated		
Anti-Sucrase-Isomaltase		
CellLine		
Caco-2		
HTB-7		
Chemical		
2,5-DHB		

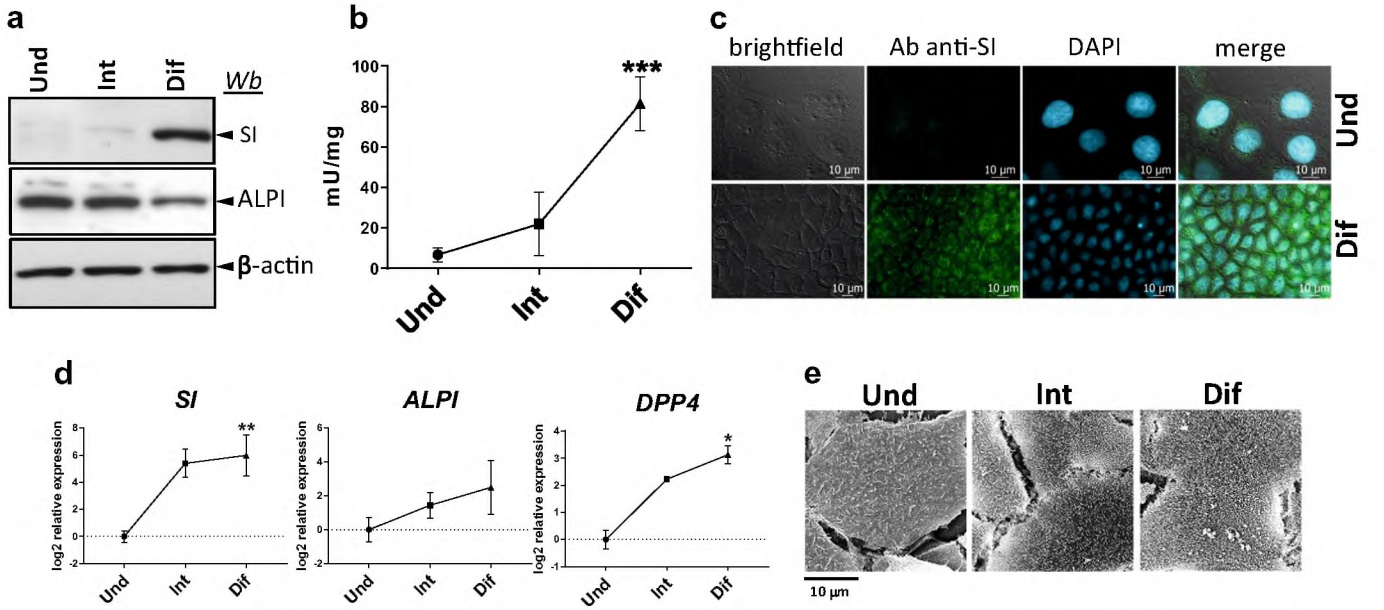

Fig. 1. Evaluation of Caco-2 cells differentiation during long term culture. Cells were analyzed at subconfluency (undifferentiated; Und), 4 days after reaching the confluence (intermediate state; Int) and 12 days post-confluency (differentiated; Dif). a Western blot analysis of the expression of brush-boarder enzymes in total cell homogenates: sucrase-isomaltase (SI) and intestinal alkaline phosphatase (ALPI); β-actin detection was used as a loading control. b Alkaline phosphatase activity measured in total cell homogenates. c Detection of sucrase-isomaltase (SI) on the cell surface of undifferentiated and differentiated Caco-2 cells by immunofluorescence microscopy. d RQ-PCR analysis of the expression of brush-boarder markers mRNA: *SI* (sucrase-isomaltase), *ALPI* (intestinal alkaline phosphatase), *DPP4* (dipeptidyl peptidase 4). The markers expression was normalized to *GAPDH* and presented in relation to undifferentiated cells in log2 scale. e SEM microphotographs of apical surface of Caco-2 monolayers at different stages of culture. Quantitative results are presented as means ($n = 3$) ± standard deviation and statistical analysis was performer by the use of Student's *t*-test (*$p < 0.05$, **p < 0,01, ***$p < 0.001$).

2,5-Dihydroxybenzoic acid
2-AB
2-Aminobenzamide
2-Mercaptoethanol
AA
Acetonitrile
ACN
Acrylamide
Alkyne
Amino Acids
Ammonium hydroxide
Amphotericin B
Anthranilic acid
Azido
Bisacrylamide
Brillant Blue
Carbohydrates
CO_2
Dimethyl sulfoxide
DMSO
DPBS
Ethanol
Formaldehyde
Formic acid
Glutaraldehyde phosphate
Glycine
Gold
Hoechst 33342
Immobilon
L-Glutamine
ManNAz
NaCl
***N*-Azidoacetylmannosamine**
NP-40
p-Nitrophenyl phosphate
Phosphate
Phosphate-buffered saline
p-Nitrophenyl
p-NP
p-NPP
Sodium acetate
Sodium carbonate
Sodium cyanoborohydride
Sodium dodecyl sulfate
Sodium phosphate
Streptomycin
TEMED
TFA
Trifluoroacetic acid
Tris-HCl
Trizma
ProteinPeptide
ALPI
Beta-actin
Peroxidase
Proteins

3. Results

3.1. Establishing the Caco-2 model of differentiation towards enterocyte-like cells

Caco-2 cells were grown in standard conditions on the plastic surface to spontaneously differentiate into enterocyte-like cells after reaching the confluence [48]. To avoid the effect of variations in cell density during seeding, the cells were analyzed in relation to time after reaching the confluence. Three time points were chosen to reflect: a) undifferentiated state (sub-confluent cells, at about 80% confluency), b) partially differentiated cells (intermediate state, 4 days after reaching the confluence) and c) fully differentiated (12 days after reaching the confluence). At each of these time points, the cells were analyzed in detail to confirm their differentiation status. At first, the expression of well-known differentiation markers was evaluated. The sucrase-isomaltase (SI) was strongly upregulated during differentiation as measured by qPCR and Western Blot, with very low levels at sparse culture and significant high expression 12 days post-confluence (Fig. 1a and d). At mRNA level, the 12 days post-confluent cells presented almost 64 times higher expression of SI gene (Fig. 1d). The intestinal alkaline

phosphatase (ALPI) expression at mRNA and protein level was not that evidently upregulated during the time of the culture (Fig. 1a and d). However, the activity of ALPI measured in cell homogenates was dramatically increasing, from barely detectable levels in sub-confluent cells to 12-fold increase after reaching 12th day post-confluency (Fig. 1b). Taken together these data suggested the formation of functional microvilli in the studied model. The immunofluorescence microscopy showed an evident increase in the presence of SI on the cell membrane in post-confluent cells (Fig. 1c). Finally, to evaluate the formation of microvilli on apical membranes, scanning electron microscopy (SEM) was performed. In sub-confluent cells, there were only irregular processes visible on apical membranes and during differentiation, a typical brush border was formed, with a growing number of microvilli which covered the entire surface of apical cell membrane 12 days post-confluence (Fig. 1e). Basing on these data, for further experiments sub-confluent Caco-2 cells were treated as undifferentiated (control cells) and cells 12 days post-confluence as fully differentiated, enterocyte-like cells.

3.2. HILIC-HPLC analysis of N-glycans derived from cell lysate proteins and secreted proteins

To describe the glycosylation changes upon differentiation, as an initial study we performed HILIC-HPLC of 2-AB labeled N-oligosaccharides derived from proteins precipitated from cell homogenates (*glycoproteome*) and from concentrated cell culture media (*glycosecretome*). The cell lysis procedure used in this study allows the *glycoproteome* fraction to contain cytoplasmic proteins as well as all membrane compartments, thus including the membrane proteins of the ER and Golgi apparatus, allowing to capture also potential changes at the initial stages of the glycosylation pathway. The second fraction which we analyzed (*glycosecretome*) allows studying of glycosylation changes which are the result of the modulation of the whole glycosylation machinery along the secretory pathway.

As a result of HILIC-HPLC analyses, we identified 14 major peaks within the chromatograms presenting both *glycoproteome*-derived N-glycans (Fig. 2; *peaks 1–14*) and *glycosecretome*-derived oligosaccharides (Fig. 3; *peaks A-N*). The chromatographic data of these analyses are summarised in Supplementary Table 2, where the Oxford Notation was used for structure names.

In the case of *glycoproteome* N-glycans analysis, the most abundant were 5 peaks *4,6,10,12* and *13* with GU values of 6.18, 7.06, 7.95, 8.79 and 9.50, respectively (Fig. 2). Basing on the GU values and exoglycosidase treatment effects, these peaks were annotated as oligomannose species (M5-M9). The comparison of peak intensities between undifferentiated and differentiated cells revealed the quantitative differences within these structure types, suggesting the downregulation of bigger structures (*peak 12* - M8 and *peak 13* - M9) and upregulation of smaller ones (*peak 4* - M5 and *peak 6* - M6) during differentiation. Other peaks were identified mainly as paucimannosidic structures (*peak 1,2 and 3*) and di- or triantennary complex oligosaccharides with or without fucose (*e.g. peak 7,8,9* and *11*).

In case of *glycosecretome*-derived N-glycans there were 4 major peaks present at GUs 7.80, 8.39, 8.81, and 9.21 (*peak G,J,K* and *L*, respectively), which were annotated as complex structures with terminal galactose residues (*peak G* - F(6)A3G2 and *J* - A3G3) and fucosylated and monosialylated complex glycans with three or four antennae (*peak K* - F(6)A2BG2S1 and *peak L* - *F(6)A3BG3S1*) (Fig. 3). Basing on the GU values, the glycans under peaks *G, I, K* and *L* are possibly bisected structures. A quantitative comparison of peak intensities between samples derived from undifferentiated and differentiated cells suggested the downregulation of *peak J* (GU 8.39; A3G3) and upregulation of *peak B* (GU 6.69; FA2G1), *C* (GU 7.04; FA2BG1) and *G* (GU 7.80; FA2BG2), which indicates a higher intensity of fucosylation of secreted glycoproteins upon differentiation of Caco-2 cells. Basing on GU values and exoglycosidases treatment effects, the other peaks were annotated mostly as complex diantennary N-glycans with terminal galactose residues with or without fucose. The oligomannose glycans were present

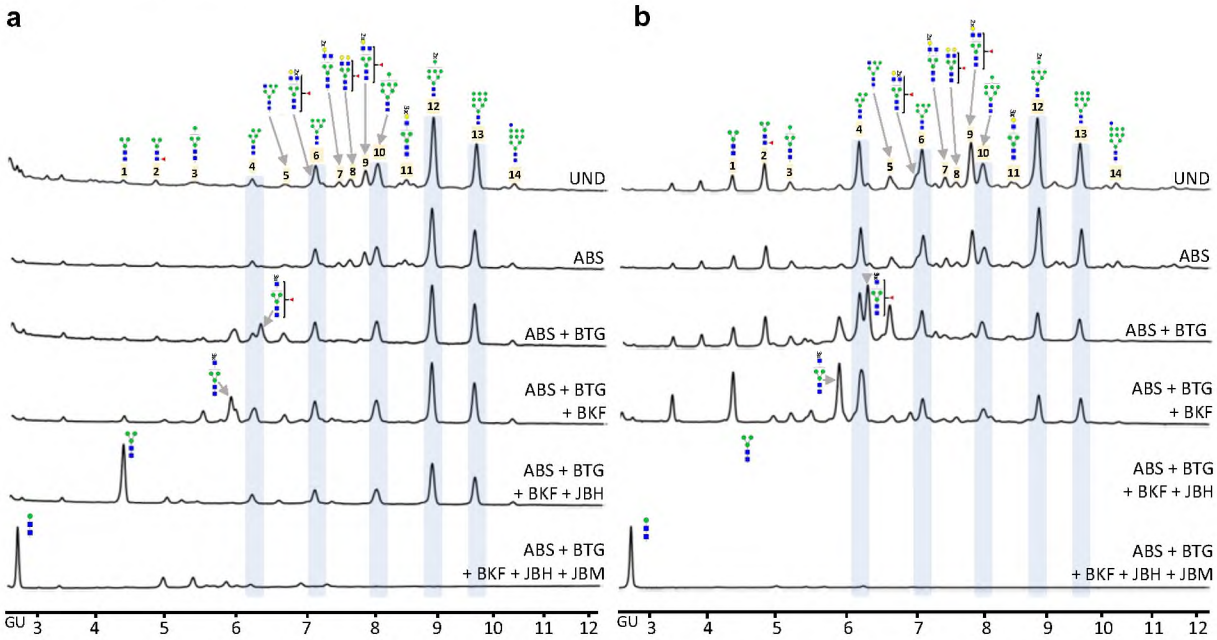

Fig. 2. NP-HPLC analysis of 2AB-labeled N-glycans released from *glycoproteome* (total cell lysate glycoproteins) of undifferentiated (a) and differentiated (b) CaCo-2 cells. The chromatogram was manually devided into 14 (1–14) separate peaks. Glycan samples were analyzed undigested (UND) and then were sequentially digested with exoglycosidases: *Arthrobacter ureafaciens* sialidase (ABS), bovine testes β(1–3,4)-galactosidase (BTG), bovine kidney α(1–2,3,4,6)-fucosidase (BKF), jack bean β-*N*-acetylhexosaminidase (JBH) and jack bean α(1–2,3,6)-mannosidase (JBM). Glycan peaks were externally standarised to glucose units (GU) and the annotation of the N-glycan structures was based on GlycoStore database comparison, exoglycosidase digestions and common knowledge of glycobiology. In some cases structural isomeres are possible. Positions of oligomannose glycans (M5-M9) are shaded in light blue. Glycan schemes were prepared using GlycoWorkbench. Red triangle, fucose; yellow circle, galactose; green circle, mannose; blue square, *N*-acetylglucosamine; purple diamond, sialic acid.

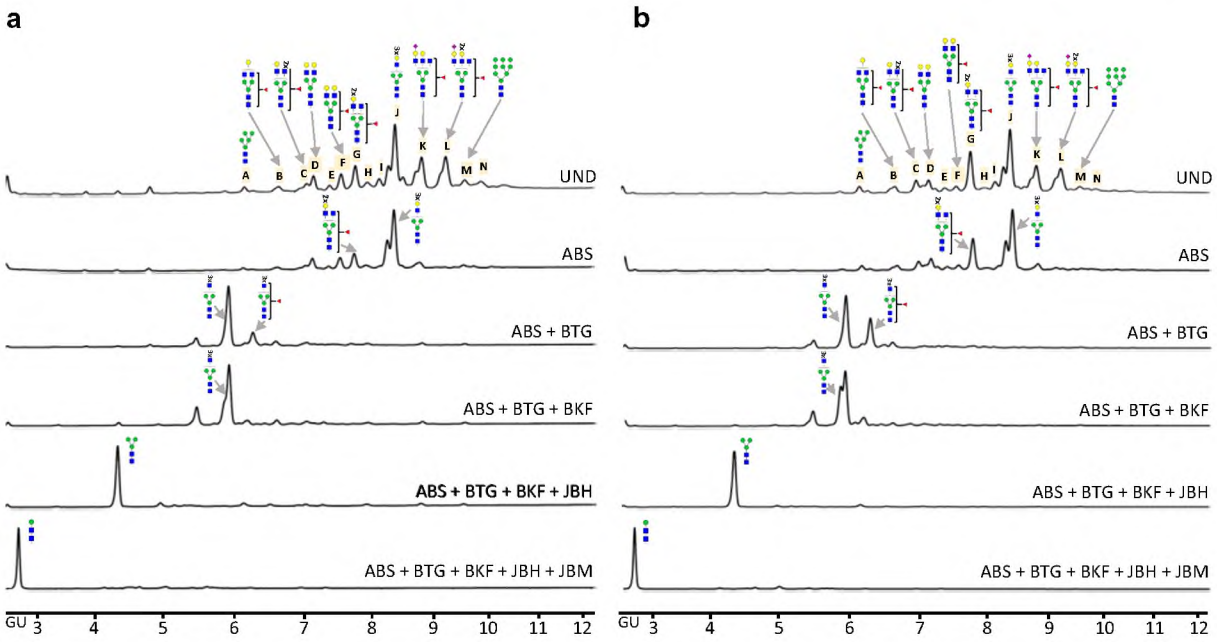

Fig. 3. NP-HPLC analysis of 2AB-labeled N-glycans released from *glycosecretome* of undifferentiated (a) and differentiated (b) CaCo-2 cells. The chromatogram was manually devided into 14 (A-N) separate peaks. Glycan samples were analyzed undigested (UND) and then were sequentially digested with exoglycosidases: *Arthrobacter ureafaciens* sialidase (ABS), bovine testes β(1–3,4)-galactosidase (BTG), bovine kidney α(1–2,3,4,6)-fucosidase (BKF), jack bean β-*N*-acetylhexosaminidase (JBH) and jack bean α(1–2,3,6)-mannosidase (JBM). Glycan peaks were externaly standarised to glucose units (GU) and the annotation of the N-glycan structures was based on GlycoStore database comparison, exoglycosidase digestions and common knowledge of glycobiology. In some cases structural isomeres are possible. Glycan schemes were prepared using GlycoWorkbench. Red triangle, fucose; yellow circle, galactose; green circle, mannose; blue square, *N*-acetylglucosamine; purple diamond, sialic acid.

at minute levels in *glycosecretome* fraction (*e.g. peak A* – M5 and *peak M* – M9).

3.3. Qualitative and quantitative analysis of glycosylation changes by mass spectrometry

For detailed qualitative and quantitative analysis of N-glycans, AA-labeled oligosaccharides from undifferentiated and differentiated cells and both protein fractions were further purified and analyzed by MALDI-TOF-MS (Figs. 4 and 5). The glycans identification was based on *m/z* values measured in the negative ion reflectron mode and common knowledge of glycobiology. The detailed structural annotation of glycans is summarised in Supplementary Table 3. The Consortium for Functional Glycomics (CFG) notation was used for the graphic representation of N-glycans with, in most cases no specification of the linkage position of monosaccharides for isomeric structures. Relative intensities of each glycan were determined using the area under the peak calculation, and the statistically significant changes between mean glycan abundances were tested by a two-tailed, unpaired *t*-test.

In general, 104 different N-glycan structures were identified. In the case of *glycoproteome* analysis, 96 glycan species were characteristic for undifferentiated cells and 103 compounds for differentiated ones. Analysis of *glycosecretome* revealed 77 N-glycans present in undifferentiated Caco-2 cells and 82 after differentiation. This observation suggests the increasing in N-glycome diversity as a result of differentiation towards enterocyte-like cells.

For quantitative comparison of glycan abundances, 9 subgroups were created basing on the sum of signals from individual species. These include paucimannosidic, oligomannose, hybrid, complex, sialylated, fucosylated, diantennary, triantennary and multiantennary N-glycans (Fig. 6 and Supplementary Table 3). *Glycoproteome* fraction analysis revealed that the majority of glycans both in undifferentiated and differentiated cells were di- and triantennary, fucosylated complex structures (Fig. 6a). The second biggest group of compounds in both cell types were oligomannose glycans (approx. 30% of all structures). The paucimannosidic, hybrid, multiantennary and sialylated oligosaccharides were also present but their abundance did not exceed 10% of all N-glycans for each. The quantitative comparison of glycan subgroups between undifferentiated and differentiated cells showed the significant upregulation of sialylation, the increment in paucimannosidic structure level and downregulation of diantennary glycans abundance in enterocyte-like cells.

The *glycosecretome* fraction analysis revealed, that all the mentioned subgroups of structures were also present, but in different proportions (Fig. 6b). In this case, the vast majority of glycans both in undifferentiated and differentiated cells were complex structures (approx. 80% of all N-glycans), mostly triantennary with a high level of fucosylation. The oligomannose structures were at minute levels (2% and 4% of all glycans for undifferentiated and differentiated cells, respectively), similarly as paucimannosidic and sialylated species. The quantitative comparison of glycan subgroups content between undifferentiated and differentiated cells showed the significant increment of oligomannose structures abundance and evident upregulation of fucosylation during differentiation (from 40% in undifferentiated cells to approx. 70% in differentiated ones).

As the second part of this study, we performed a comparative analysis of individual N-glycan species expression for both protein fractions separately. The most abundant compounds (average relative amount > 1.0%) together with their relative abundances in both protein fractions are summarised in Figs. 4c and 5c. The major peaks within the N-glycome of the *glycoproteome* fraction derived from control and differentiated cells were identified as oligomannose structures M5 (H5N2-AA), M6 (H6N2-AA), M7 (H7N2-AA), M8 (H8N2-AA) and M9 (H9N2-AA), with *m/z* 1354.60, *m/z* 1516.60, *m/z* 1678.64, *m/z* 1840.71 and *m/z* 2002.80, respectively (Fig. 4, Supplementary Table 3). This is in-line with the data from HILIC-HPLC analysis, where these structures were also identified as major peaks within the chromatogram (Fig. 2). The quantitative comparison of the expression of

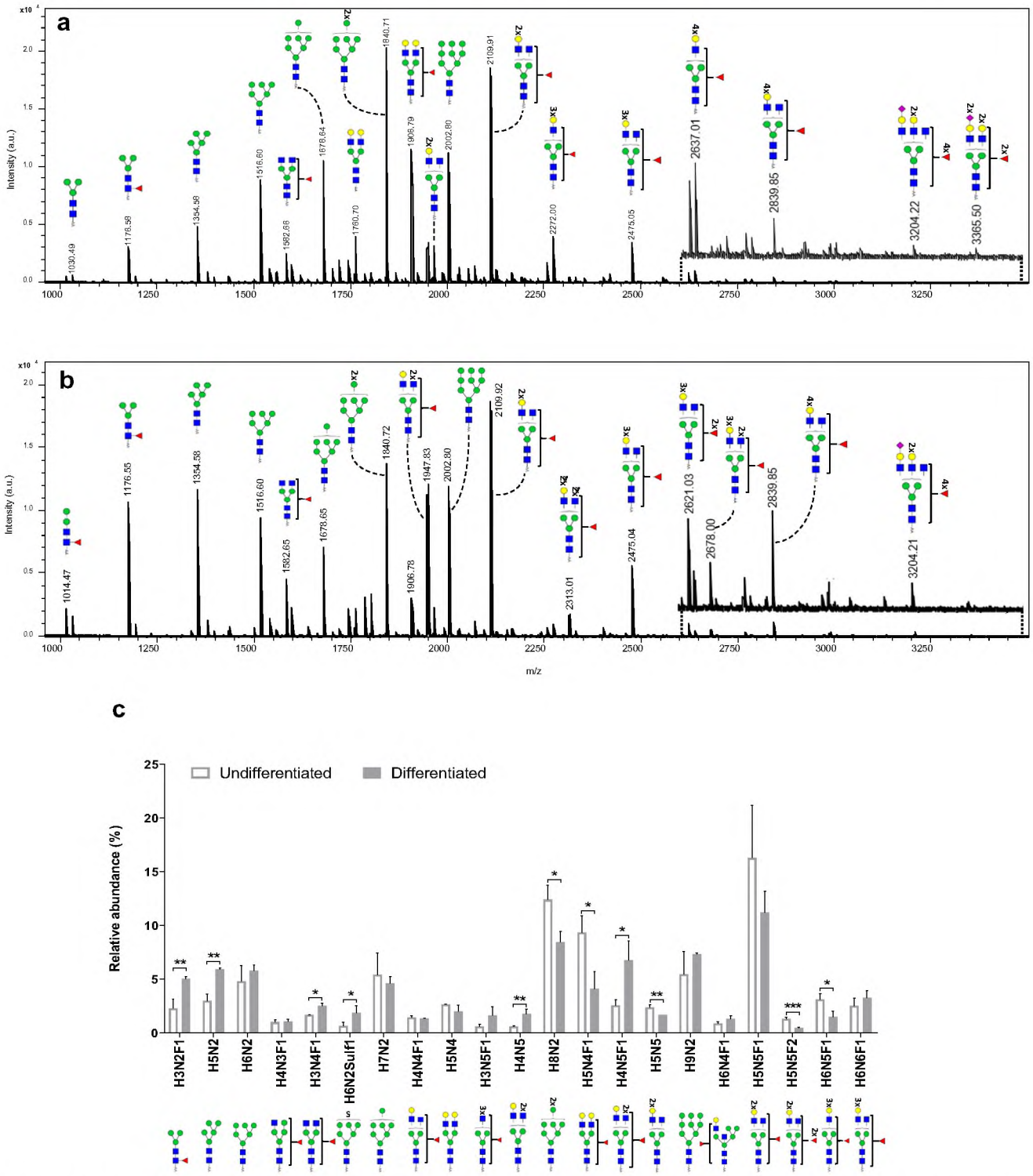

Fig. 4. MALDI-TOF-MS analysis of AA-labeled N-glycans released from *glycoproteome* (total cell lysate glycoproteins) of undifferentiated (a) and differentiated (b) CaCo-2 cells. Glycan samples were analyzed in negative-ion reflectron mode. The composition of the N-glycan structures was deduced from the *m/z* values and common knowledge of glycobiology. Only major structures are depicted and the complete annotation of MS spectra is presented in Supplementary Table 3. In some cases structural isomers are possible. Glycan schemes were prepared using GlycoWorkbench. Red triangle, fucose; yellow circle, galactose; green circle, mannose; blue square, *N*-acetylglucosamine; purple diamond, sialic acid; a.u., arbitrary units. **c** The comparison of relative amounts of most abundant (≥1%) glycan species from undifferentiated and differentiated cells. Results are presented as means (n = 3) ± standard deviation and significant differences were assessed by using Student *t*-test (*$p < 0.05$, **$p < 0.01$, ***$p < 0.001$). H, hexose; *N*, *N*-acetylhexosamine; F, fucose; Sulf, sulfate.

these N-glycans between undifferentiated and differentiated Caco-2 cells revealed the significant downregulation of H8N2-AA accompanied by the upregulation of H5N2-AA, as a result of cellular differentiation (Fig. 4). The enterocyte-like cells presented also a higher content of fucosylated oligomannose structure H3N2F1-AA, detected at *m/z* 1176.55 (Fig. 4).

Other major peaks that were observed in the *glycoproteome* fraction were detected at *m/z* 1582.66, *m/z* 1760.70, *m/z* 1906.79, *m/z*

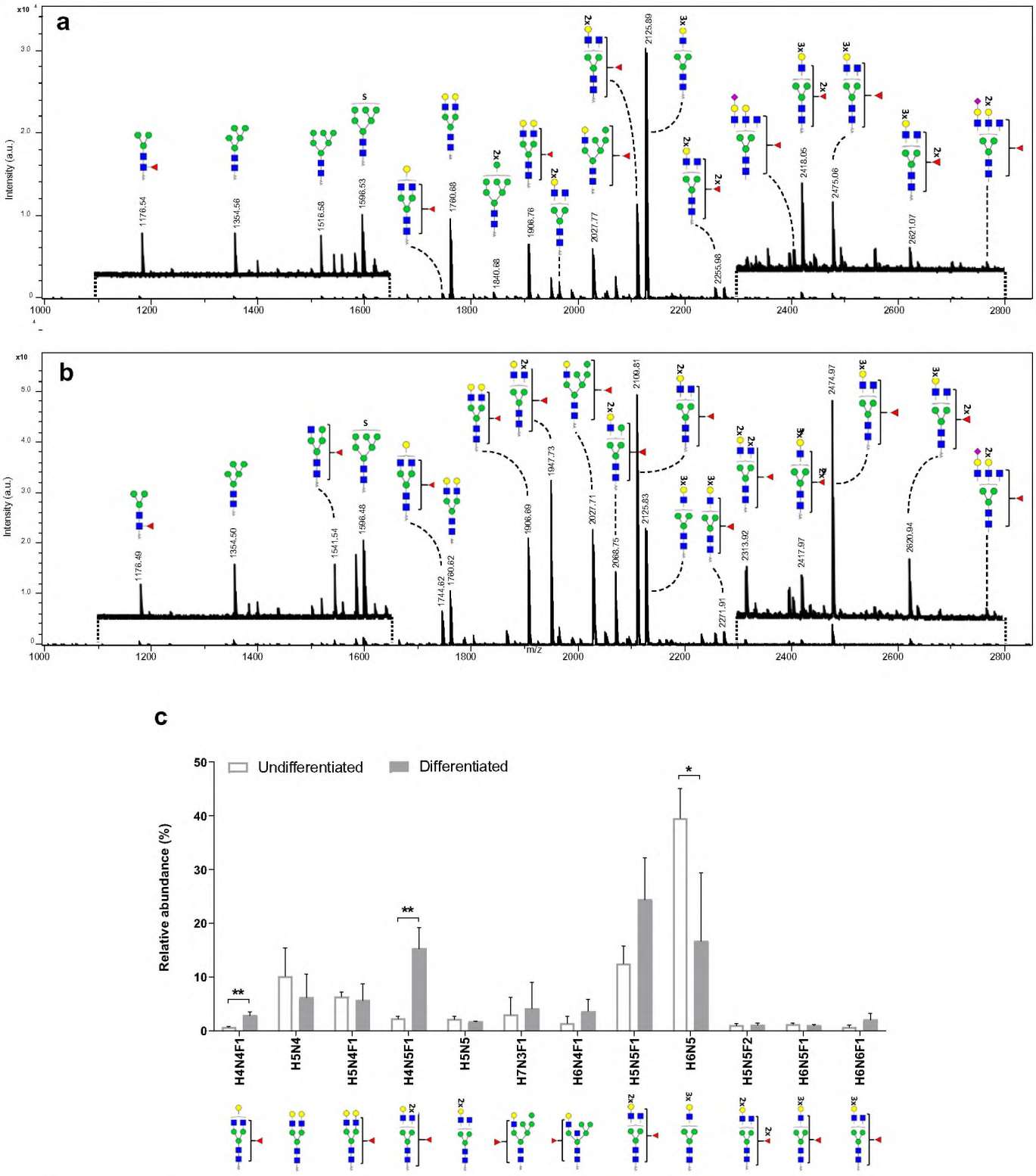

Fig. 5. MALDI-TOF-MS analysis of AA-labeled N-glycans released from *glycosecretome* of undifferentiated (a) and differentiated (b) CaCo-2 cells. Glycan samples were analyzed in negative-ion reflectron mode. The composition of the N-glycan structures was deduced from the *m/z* values and common knowledge of glycobiology. Only major structures are depicted and the complete annotation of MS spectra is presented in Supplementary Table 3. In some cases structural isomeres are possible. Glycan schemes were prepared using GlycoWorkbench. Red triangle, fucose; yellow circle, galactose; green circle, mannose; blue square, *N*-acetylglucosamine; purple diamond, sialic acid; a.u., arbitrary units. c The comparison of relative amounts of most abundant (≥1%) glycan species of undifferentiated and differentiated cells. Results are presented as means (n = 3) ± standard deviation and significant differences were assessed by using Student *t*-test (*$p < 0.05$, **$p < 0.01$, ***$p < 0.001$). H, hexose; *N*, *N*-acetylhexosamine; F, fucose.

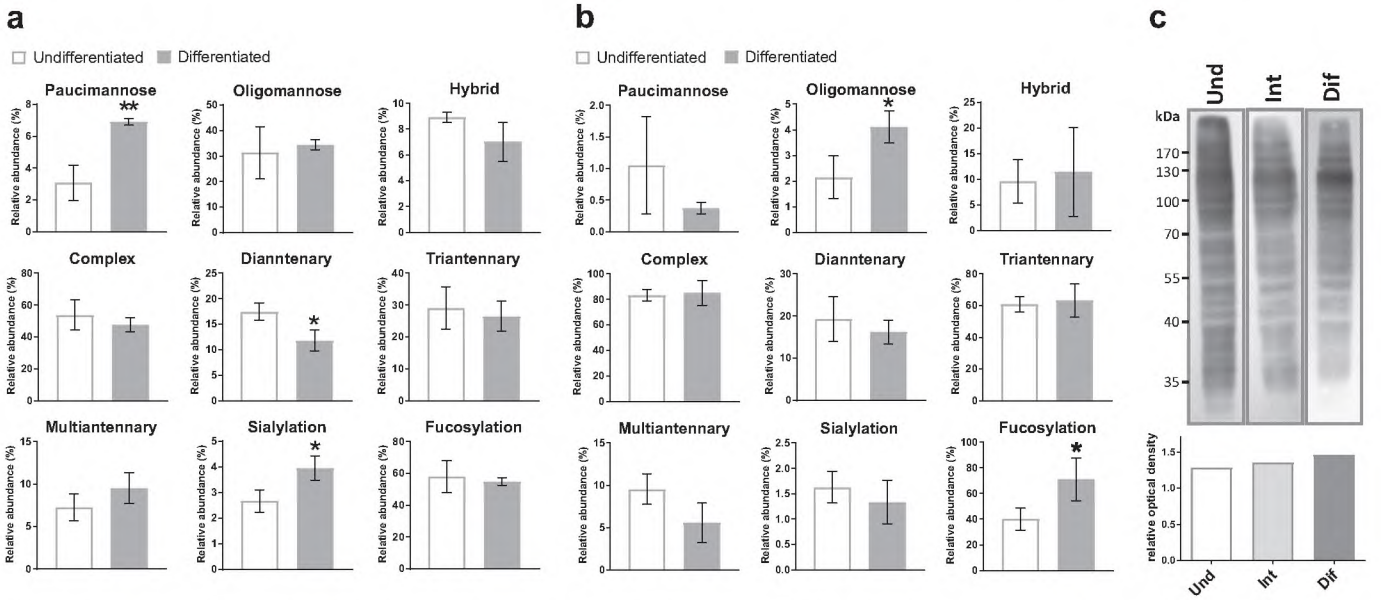

Fig. 6. Comparison of N-glycosylation changes in undifferentiated (Und), intermediate (Int) and differentiated (Dif) CaCo-2 cells. AA-labeled N-glycans derived from *glycoproteome* (a) and *glycosecretome* (b) were analyzed by MALDI-ToF-MS. The mean relative abundances of glycan structures of the same type were grouped together. Results are presented as means (n = 3) ± standard deviation and significant differences between undifferentiated and differentiated cells were assessed by using Student *t*-test (*$p < 0.05$, **$p <$ 0,01). Glycoproteins isolated from cells fed with Ac_4ManNAz were coupled to biotin-alkyne by *"click"* chemistry and then resolved by SDS-PAGE. Sialoglycoproteome was visualized on membrane by chemiluminescence, after incubation with streptavidin-HRP (c). Optical density of each visualized lane was normalized to the corresponding CBB staining.

1947.83, *m/z* 2109.91, *m/z* 2272.00.88, *m/z* 2313.01 and *m/z* 2475.04. These peaks were mainly di- or triantennary, galactosylated and fucosylated complex oligosaccharides. This observation was in line with the HPLC data, where these species were also identified basing on the exoglycosidases treatment (Fig. 2). Among these glycans, the structures at *m/z* 1582.66 (H3N4F1-AA), *m/z* 1801.78 (H4N5-AA) and *m/z* 1947.83 (H4N5F1-AA) were significantly upregulated in differentiated cells, whereas glycans at *m/z* 1906.79 (H5N4F1-AA), *m/z* 1963.86 (H5N5-AA) and *m/z* 2256.03 (H5N5F2-AA) were at significantly lower amounts after differentiation, suggesting that differentiation process resulted in the rearrangement of complex N-glycan pool (Fig. 4). The most apparent change of this type was the evident downregulation of diantennary, fucosylated fully galactosylated glycan H5N4F1-AA (approx. 9% in undifferentiated cells *vs.* approx. 4% in differentiated ones) and upregulation of triantennary or bisected diantennary, fucosylated and partially galactosylated structure H4N5F1-AA (approx. 2,5% *vs.* approx. 7%, respectively) (Fig. 4c).

The glycomic analysis of the *glycosecretome* fraction revealed, similarly to an HPLC approach the negligible involvement of oligomannose glycans within the N-glycan pool (Fig. 5). Although the total oligomannose structures abundance was statistically upregulated upon Caco-2 cells differentiation (Fig. 6b) none significant differences were detected when individual species were considered (Fig. 5c). The major peaks within the MALDI-MS spectrum of N-glycans derived from this protein fraction were identified at *m/z* 1744.62, *m/z* 1760.68, *m/z* 1906.76, *m/z* 2027.77 *m/z* 2068.75, *m/z* 2109.81 and *m/z* 2125.89 and were annotated mainly as di- or triantennary, galactosylated and fucosylated complex structures (Fig. 5). This was in line with the HPLC data, where these species were also identified basing on exoglycosidases treatment (Fig. 3). Among these peaks, one was identified as fucosylated, hybrid glycan with 6 mannose residues and galactosylated antenna (*m/z* 2027.77; H7N3F1-AA) (Fig. 5). The significant quantitative differences of N-glycans from *glycosecretome* between undifferentiated and enterocyte-like cells concerned three species (Fig. 5c). We observed an evident decrease of the most intense signal at *m/z* 2125.89 after differentiation, which represented the dramatic downregulation of triantennary, fully galactosylated complex N-glycan (approx. 40% down to approx. 17%). The other significant changes that we observed were: an increased abundance of fucosylated, monogalactosylated diantennary complex structure (H4N4F1-AA) at *m/z* 1744.62 and upregulation of fucosylated, monogalactosylated triantennary or bisected diantennary complex structure (H4N5F1-AA) at *m/z* 1947.73 as a result of differentiation.

Finally, we found qualitative differences between the N-glycomes of undifferentiated and differentiated Caco-2 cells (Supplementary Table 3). Within the *glycoproteome* fraction, the most evident was the identification of H5N6-AA glycan at *m/z* 2166.90 only in case of fully differentiated cells. Exclusively the latter cells presented also the expression of highly fucosylated and/or sialylated complex glycans with at least 5 hexoses and 6 N-Acetylhexosamines (H5N6), suggesting intensification of branching, fucosylation and sialylation of *glycoproteome* and *glycosecretome* during differentiation.

3.4. Analysis of cellular sialome changes during differentiation of Caco-2 cells

As the glycan analysis described above revealed a significant intensification of glycoproteome sialylation as a result of differentiation of Caco-2 cells, we analyzed the cellular sialome employing metabolic labeling of sialic acid with "click" chemistry for visualization. The cells were cultured with the presence of azide-modified sialic acid precursor (ManNAz) and sialoglycoproteins were visualized on PVDF membrane after electrophoretic resolving of cell lysate proteins derived from undifferentiated, intermediate and differentiated cells (Fig. 6c). The relative optical density of protein bands of differentiated cells was higher, suggesting an intensification of sialylation during differentiation. The observed changes concerned especially a protein band of about 130 kDa. As this method is not specific for N-glycans but rather for all types of protein-attached glycan epitopes we cannot conclude, that this change is a result of an intensification of sialylation of N-glycans exclusively.

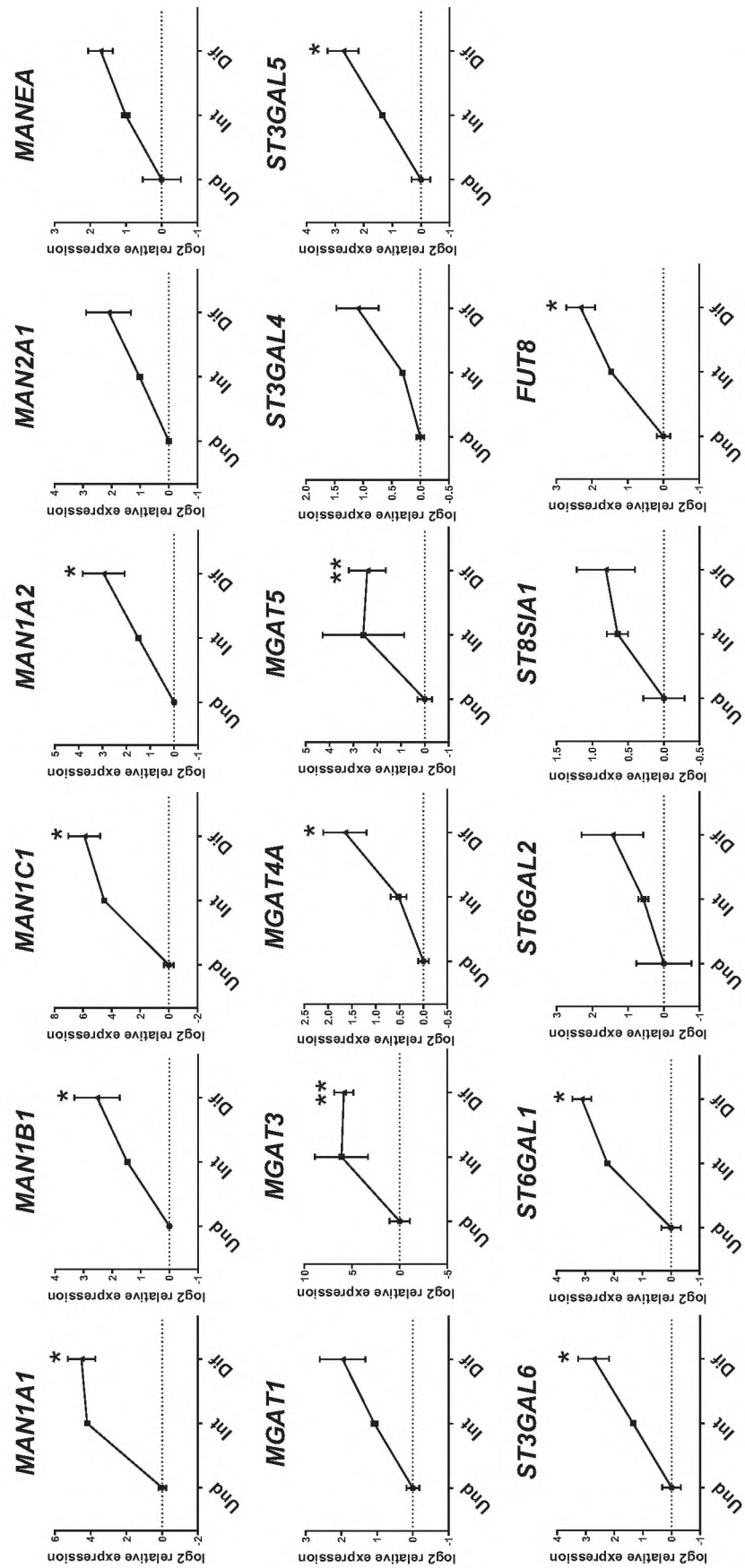

Fig. 7. RQ-PCR analysis of the expression of glycosylation pathway enzymes mRNA in undifferentiated (Und), intermediate (Int) and differentiated (Dif) CaCo-2 cells. The genes expression was normalized to *GAPDH* and presented in relation to undifferentiated cells in log2 scale. Results are presented as means (n = 3) ± standard deviation and significant differences were assessed by using Student *t*-test ($^{*}p < 0.05$).

3.5. Changes of N-glycosylation pathway - related genes expression during differentiation

The RNA isolated from undifferentiated, intermediate and differentiated cells was analyzed using RT-qPCR in terms of changes of the expression of genes encoding key glycosylation enzymes (Fig. 7). We studied four groups of genes, which are responsible for: i) trimming of oligomannose glycans at the initial steps of the N-glycosylation pathway (MAN1A1, MAN1A2, MAN1B1, MAN1C1, MAN2A1 and MANEA); ii) branching of N-glycans (MGAT1, MGAT3, MGAT4A and MGAT5); iii) fucosylation (FUT8) and iv) sialylation (ST3GAL4, ST3GAL5, ST3GAL6, ST6GAL1, ST6GAL2 and ST8SIA1). We observed significantly increased expression of alpha-mannosidases I in differentiated cells which is consistent with the observed remodeling of oligomannose N-glycans upon differentiation (downregulation of M8 with accompanying upregulation of M5 glycans) (Figs. 3 and 4). The most evident change in this group of genes was the upregulation of MAN1C1 expression in enterocyte-like cells. Differentiated cells were also characterized by the increased expression of MGAT3 encoding GlcNAc transferase III, responsible for the formation of "bisected" N-glycan species. Also, other "branching" enzymes (MGAT4A and MAGT5) were upregulated in enterocyte-like cells. All these changes can be possibly responsible for the observed altering of complex oligosaccharides during differentiation which we described above. Finally, the differentiated cells were characterized by the upregulation of FUT8, ST3GAL6 and ST6GAL1 expression. These changes are in line with our glycomic data which showed the intensification of fucosylation and sialylation of glycosecretome and glycoproteome, respectively, during differentiation towards enterocyte-like cells (Figs. 3 and 4).

4. Discussion

In this study, we investigated the N-glycosylation profiles of two protein pools (cell lysate proteins – glycoproteome and secreted proteins – glycosecretome), derived from differentiating Caco-2 human adenocarcinoma cells. N-glycomes as well as expression of glycosylation-related genes of undifferentiated and differentiated cells were compared. The differentiation status of Caco-2 cells at 12th day post-confluency was analyzed and enterocyte-like phenotype was confirmed at biochemical (high expression of SI and high activity of ALPI in vitro) and morphological (microvilli formation visualized by electron microscopy) level. This is consistent with several studies in which the fully differentiated cells are analyzed at about 21th day of culture [37,49]. In our experiments, we refer to the time after reaching the confluence and 12 days post-confluent cells were on average cultured for about 20 days after seeding. In general, we believe that analyzing Caco-2 cells in relation to the time of reaching the full intracellular contact in vitro is more legitimate since the differentiation process only starts when cells reach confluence. In addition, it eliminates an error resulting from an uneven number of cells at seeding and the influence of other factors potentially modifying the rate of cell proliferation and differentiation [50].

Analysis of the abundance of main N-glycans structure types revealed the domination of complex structures, relatively high content of oligomannose oligosaccharides and low concentration of hybrid species before, as well as after differentiation. In general, this quantitative distribution of main glycan traits of Caco-2 glycoproteome is in line with the previous analysis of cell lysate-derived glycoproteins published by Holst et al. [51], who however did analyze only undifferentiated cells.

The N-glycomic analyses showed a substantial remodeling in the glycan repertoire of both protein pools as a result of differentiation. To be sure, that the changes observed are the result of the differentiation process itself, we compared the HPLC profiles of N-glycans derived from undifferentiated, intermediate and differentiated CaCo-2 cells (Supplementary Fig. 1). We observed an evident trend in upregulation of H5N2 (M5) glycan and in downregulation of H8N2 (M8) glycan during differentiation.

The detailed glycan analyses made by MALDI-MS and HPLC showed, that the most apparent change was the upregulation of fucosylation in differentiated cells and this effect was visible at the global level only within the glycosecretome-derived N-glycans. The individual glycan analysis revealed that glycoproteins secreted from differentiated cells possess higher content of species such as H4N4F1, H4N5F1 and H5N5F1. One of these structures (H4N5F1) was also significantly elevated in the whole cell lysate-derived glycoproteome pool from differentiated cells. The GU values and exoglycosidases treatment effects allows us to claim that these fucosylated structures are bisected N-glycans. This corresponds with the fact that as a result of differentiation we observe an upregulation of the expression of FUT8 encoding α1,6-fucosyltransferase, responsible for core-fucosylation of N-glycans, as well as the elevation of MGAT3 transcript encoding β1,4-N-acetylglucosaminyltransferase III (GnT-III) which is responsible for the introduction of a bisecting GlcNAc residue. Despite we do not see any global upregulation of fucosylation within the glycoproteome fraction during differentiation, the individual structure analysis revealed that differentiated cells possess higher amounts of some fucosylated species, with unusual fucosylated paucimannosidic structure (H3N2F1) among others, suggesting that strengthening of global fucosylation potential is indeed associated with differentiation process. Studies of Park et al. describe a similar effect on cell membrane-derived proteins where the fucosylation and the amount of bisected structures were significantly elevated during differentiation of Caco-2 cells [37]. Holst et al. showed recently, that fucosylation is associated with the expression of intestinal differentiation markers, such as the homeobox gene CDX1 and villin in colorectal cancer cell lines [51]. Many data prove that the fucosylation status of gastrointestinal tract epithelium is essential for its proper functions. Studies described by Wang et al. clearly shows that the abrogation of de novo synthesis of GDP-fucose and consequent fucosylation deficiency lead to colitis, dysplasia and eventually adenocarcinoma in mice, which is probably dependant on the loss of Notch activation and downregulation of Hes1 transcription factor [52]. Moreover, fucosylation of GI tract epithelia is known to be a crucial player of the host-microorganisms interactions [53]. It is also known, that fucosylated glycoconjugates serve as a source of L-fucose for microbial energy harvest and some glycoproteins are shed into the intestinal lumen for this purpose (with brush border marker enzymes, such as SI among others) [54]. The studies mentioned above proves, that fucosylation of IECs is dynamic process and expression of some fucosyltransferases can be modulated by bacteria itself or by intrinsic pro-inflammatory signals. In this context, the proper formation of fucosylated glycoconjugates during IECs differentiation is crucial for maintaining the integrity of intestinal mucosa but also for delivering the interaction points with natural microflora. The proper regulation of glycosylation in these cells is also important as some glycan epitopes are recognized by pathogens [21]. The formation of bisected N-glycans due to the elevated expression of MGAT3 is probably important for the formation of proper adhesion relations within the intestinal epithelium. Considering the differentiation model presented here some reports suggests, that these type of glycosylation is involved in the regulation of Mesenchymal-Epithelial-Transition (MET), especially in the context of a modification of E-cadherin glycosylation with bisecting GlcNAc moiety [55].

In our study the differentiation of Caco-2 cells was accompanied by the elevation of sialylation which can result from the upregulation of ST6GAL1 and ST3GAL6 genes expression encoding sialyltransferases responsible for the addition of sialic acid in α2,6 and α2,3 linkage, respectively. This effect was observed in whole cell glycoproteome pool and is in line with previous reports [37]. We also observed a slight elevation of the signal derived from sialoproteome of whole cell lysate when we analyzed metabolically labeled differentiating Caco-2 cells. The presence of sialylated glycoepitopes on maturated intestinal epithelia is broadly associated with the mechanism of pathogen-host

interactions. Sialic acid is known to be recognized by parasitic protists [56], pathogenic bacteria [57,58], viruses [59] and bacterial toxins [60], and regulation of its expression can be considered as an important part of host defense mechanisms.

Finally, we observed a substantial change within oligomannose glycan repertoire when glycoproteome pool was analyzed. Although, the total content of this type of glycans did not change after differentiation, at the individual glycan level we did notice an evident switch from bigger structures (H8N2) towards the formation of smaller ones (especially H5N2), suggesting the augmentation of mannose trimming at the initial steps of glycosylation pathway. This was supported by the analysis of the expression of mRNAs encoding Golgi alpha mannosidases, where as a result of differentiation we observed strong upregulation of MAN1C1 but also MAN1A1, MAN1A2 and MAN1B1. Remodeling of oligomannose glycans content is broadly observed in studies concerning cellular differentiation [18,61,62]. In the previously mentioned study, Park et al. describes significant downregulation of these type of glycans, when membrane-bound glycoproteins were analyzed during differentiation [37]. In our studies, thanks to pooling the glycoproteins not only from the plasma membrane but also derived from intracellular membrane compartments (ER and Golgi apparatus) within the glycoproteome fraction, we were able to track the remodeling of the oligomannose structures also at the initial steps of N-glycosylation pathway. In our opinion, the augmented mannose trimming during differentiation of Caco-2 cells not only results in downregulation of oligomannose species on maturated membrane-bound glycoproteins, which was observed by Park et al., but also serves as a substrate-delivery process, which is required for the formation of more complex repertoire of N-glycans on secreted and membrane proteins.

Basing on our observations, we assume that the glycosecretome pool (similar as the cell surface glycoproteins) consists of proteins that undergo full glycosylation process along secretory pathway thus representing a final picture of fully matured glycans. Here, the comparison of the glycosylation status of these proteins with the glycoproteome from the total cell lysate and recently published membrane-bound glycoproteins analysis revealed the substantial differences in qualitative and quantitative glycans distribution between these three fractions. Thus, to describe the complex glycobiological status of cell physiology in vitro we suggest to analyze these three glycomes separately. This is extremely important especially when the studies on cell glycobiology are focused on looking for potential novel glycan-based biomarkers of disease.

In conclusion, we present here a detailed picture of glycosylation changes during intestinal epithelial cell differentiation in vitro. We hypothesize, that augmentation of mannose trimming at the initial steps of N-glycosylation process, together with the remodeling of key glycosyltransferases expression leads to increased diversity of N-glycans, enhanced fucosylation and sialylation of complex species and probable increment of glycans bisection. We also suggest H4N5F1 glycan as a potential biomarker of intestinal epithelial cell differentiation, as this structure abundance clearly increases after differentiation not only in glycoproteome pool but also when glycosecretome of Caco-2 cells was analyzed. It is now important to address the question of whether (or which of) these glycosylation changes are the drivers of intestinal cell differentiation or are the consequence of changing intercellular relations during the differentiation process. An attempt to answer these questions needs definitely further, detailed functional studies.

Author contributions

PLL and PP conceived the project. PLL designed all experiments, performed all glycomic studies and analyzed data. MJ cultured the cells and performed Western blots. KC performed PCRs. MP performed immunofluorescence microscopy. ALS and JB performed statistical analyses and helped preparing the figures. PLL, PP and JJ drafted the manuscript. All authors discussed the results and reviewed the manuscript.

Supplementary data to this article can be found online at https://doi.org/10.1016/j.bbamcr.2019.118555.

Transparency document

The Transparency document associated with this article can be found, in online version.

Declaration of competing interest

The authors declare that they have no conflict of interest.

Acknowledgements

We wish to thank Dr. Jolanta Łukasiewicz from Ludwik Hirszfeld Institute of Immunology and Experimental Therapy for making it possible to perform MALDI-MS analyses. We also thank Dr. Grzegorz Tylko and Dr. Michał Dykas from the Institute of Zoology and Biomedical Research of the Jagiellonian University in Kraków for assistance in SEM analyses.

Funding

This work was supported by the Polish National Science Centre (NCN), grant number UMO-2012/07/D/NZ1/00523.

References

[1] J.E. Turnbull, R.A. Field, Emerging glycomics technologies, Nat. Chem. Biol. 3 (2007) 74–77, https://doi.org/10.1038/nchembio0207-74.
[2] N.G. Jayaprakash, A. Surolia, Role of glycosylation in nucleating protein folding and stability, Biochem. J. 474 (2017) 2333–2347, https://doi.org/10.1042/BCJ20170111.
[3] A. Varki, Biological roles of glycans, Glycobiology. 27 (2017) 3–49, https://doi.org/10.1093/glycob/cww086.
[4] S.S. Pinho, C.A. Reis, Glycosylation in cancer: mechanisms and clinical implications, Nat. Rev. Cancer 15 (2015) 540–555, https://doi.org/10.1038/nrc3982.
[5] K.W. Moremen, M. Tiemeyer, A.V. Nairn, Vertebrate protein glycosylation: diversity, synthesis and function, Nat. Rev. Mol. Cell Biol. 13 (2012) 448–462, https://doi.org/10.1038/nrm3383.
[6] T.K. Noah, B. Donahue, N.F. Shroyer, Intestinal development and differentiation, Exp. Cell Res. 317 (2011) 2702–2710, https://doi.org/10.1016/j.yexcr.2011.09.006.
[7] C. Günther, H. Neumann, M.F. Neurath, C. Becker, Apoptosis, necrosis and necroptosis: cell death regulation in the intestinal epithelium, Gut. 62 (2013) 1062–1071, https://doi.org/10.1136/gutjnl-2011-301364.
[8] S. Tan, N. Barker, Epithelial stem cells and intestinal cancer, Semin. Cancer Biol. 32 (2015) 40–53, https://doi.org/10.1016/J.SEMCANCER.2014.02.005.
[9] Q. Wang, Y. Zhou, P. Rychahou, T.W.-M. Fan, A.N. Lane, H.L. Weiss, B. Evers, Ketogenesis contributes to intestinal cell differentiation, Cell Death Differ. 24 (2016) 458–468, https://doi.org/10.1038/cdd.2016.142.
[10] E.N. Elliott, K.H. Kaestner, Epigenetic regulation of the intestinal epithelium, Cell. Mol. Life Sci. 72 (2015) 4139–4156, https://doi.org/10.1007/s00018-015-1997-9.
[11] Y. Zhou, Q. Wang, Z. Guo, H.L. Weiss, B.M. Evers, Nuclear factor of activated T-cell c3 inhibition of mammalian target of rapamycin signaling through induction of regulated in development and DNA damage response 1 in human intestinal cells, Mol. Biol. Cell 23 (2012) 2963–2972, https://doi.org/10.1091/mbc.E12-01-0037.
[12] M. Yao, D.P. Zhou, S.M. Jiang, Q.H. Wang, X.D. Zhou, Z.Y. Tang, J.X. Gu, Elevated activity of N-acetylglucosaminyltransferase V in human hepatocellular carcinoma, J. Cancer Res. Clin. Oncol. 124 (1998) 27–30.
[13] Q. Wang, Y. Zhou, P. Rychahou, C. Liu, H.L. Weiss, B.M. Evers, NFAT5 represses canonical Wnt signaling via inhibition of β-catenin acetylation and participates in regulating intestinal cell differentiation, Cell Death Dis. 4 (2013) e671, , https://doi.org/10.1038/cddis.2013.202.
[14] H. Schachter, The role of the GlcNAc(beta)1,2Man(alpha)-moiety in mammalian development. Null mutations of the genes encoding UDP-N-acetylglucosamine:alpha-3-D-mannoside beta-1,2-N-acetylglucosaminyltransferase I and UDP-N-acetylglucosamine:alpha-D-mannoside beta-1,2, Biochim. Biophys. Acta 1573 (2002) 292–300.
[15] T. Yamashita, R. Wada, T. Sasaki, C. Deng, U. Bierfreund, K. Sandhoff, R.L. Proia, A vital role for glycosphingolipid synthesis during development and differentiation, Proc. Natl. Acad. Sci. U. S. A. 96 (1999) 9142–9147.
[16] R.S. Haltiwanger, J.B. Lowe, Role of glycosylation in development, Annu. Rev. Biochem. 73 (2004) 491–537, https://doi.org/10.1146/annurev.biochem.73.

011303.074043.
[17] K.M. Wilson, J.E. Thomas-Oates, P.G. Genever, D. Ungar, Glycan profiling shows unvaried N-glycomes in MSC clones with distinct differentiation potentials, Front. Cell Dev. Biol. 4 (2016) 52, https://doi.org/10.3389/fcell.2016.00052.
[18] H. Hamouda, M. Ullah, M. Berger, M. Sittinger, R. Tauber, J. Ringe, V. Blanchard, N-glycosylation profile of undifferentiated and adipogenically differentiated human bone marrow mesenchymal stem cells: towards a next generation of stem cell markers, Stem Cells Dev. 22 (2013) 3100–3113, https://doi.org/10.1089/scd.2013.0108.
[19] H. Montacir, N. Freyer, F. Knöspel, T. Urbaniak, T. Dedova, M. Berger, G. Damm, R. Tauber, K. Zeilinger, V. Blanchard, The cell-surface N-glycome of human embryonic stem cells and differentiated hepatic cells thereof, ChemBioChem. 18 (2017) 1234–1241, https://doi.org/10.1002/cbic.201700001.
[20] H. Tateno, S. Saito, K. Hiemori, K. Kiyoi, K. Hasehira, M. Toyoda, Y. Onuma, Y. Ito, H. Akutsu, J. Hirabayashi, α2–6 sialylation is a marker of the differentiation potential of human mesenchymal stem cells, Glycobiology 26 (2016) cww039, https://doi.org/10.1093/glycob/cww039.
[21] A.P. Moran, A. Gupta, L. Joshi, Sweet-talk: role of host glycosylation in bacterial pathogenesis of the gastrointestinal tract, Gut. 60 (2011) 1412–1425, https://doi.org/10.1136/gut.2010.212704.
[22] M.-C. Biol-N'garagba, P. Louisot, Regulation of the intestinal glycoprotein glycosylation during postnatal development: role of hormonal and nutritional factors, Biochimie. 85 (2003) 331–352, https://doi.org/10.1016/S0300-9084(03)00039-7.
[23] I. Chantret, A. Barbat, E. Dussaulx, M.G. Brattain, A. Zweibaum, Epithelial polarity, villin expression, and enterocytic differentiation of cultured human colon carcinoma cells: a survey of twenty cell lines, Cancer Res. 48 (1988) 1936–1942 http://www.ncbi.nlm.nih.gov/pubmed/3349466 , Accessed date: 5 October 2018.
[24] B.A. Potter, R.P. Hughey, O.A. Weisz, Role of N- and O-glycans in polarized biosynthetic sorting, Am. J. Physiol. Physiol. 290 (2006) C1–C10, https://doi.org/10.1152/ajpcell.00333.2005.
[25] D. Mo, S.A. Costa, G. Ihrke, R.T. Youker, N. Pastor-Soler, R.P. Hughey, O.A. Weisz, Sialylation of N-linked glycans mediates apical delivery of endolyn in MDCK cells via a galectin-9-dependent mechanism, Mol. Biol. Cell 23 (2012) 3636–3646, https://doi.org/10.1091/mbc.E12-04-0329.
[26] S. Angeloni, J.L. Ridet, N. Kusy, H. Gao, F. Crevoisier, S. Guinchard, S. Kochhar, H. Sigrist, N. Sprenger, Glycoprofiling with micro-arrays of glycoconjugates and lectins, Glycobiology. 15 (2005) 31–41, https://doi.org/10.1093/glycob/cwh143.
[27] F. Ulloa, F.X. Real, Differential distribution of sialic acid in alpha2,3 and alpha2,6 linkages in the apical membrane of cultured epithelial cells and tissues, J. Histochem. Cytochem. 49 (2001) 501–510, https://doi.org/10.1177/002215540104900410.
[28] A. Youakim, A. Herscovics, Differentiation-associated decrease in the proportion of fucosylated polylactosaminoglycans of CaCo-2 human colonic adenocarcinoma cells, Biochem. J. 247 (1987) 299–306 http://www.ncbi.nlm.nih.gov/pubmed/3122722 , Accessed date: 5 October 2018.
[29] I. Brockhausen, P.A. Romero, A. Herscovics, Glycosyltransferase changes upon differentiation of CaCo-2 human colonic adenocarcinoma cells, Cancer Res. 51 (1991) 3136–3142 http://www.ncbi.nlm.nih.gov/pubmed/1904002 , Accessed date: 5 October 2018.
[30] J.W. Dennis, M. Granovsky, C.E. Warren, Glycoprotein glycosylation and cancer progression, Biochim. Biophys. Acta 1473 (1999) 21–34.
[31] S. Hakomori, Glycosylation defining cancer malignancy: new wine in an old bottle, Proc. Natl. Acad. Sci. U. S. A. 99 (2002) 10231–10233, https://doi.org/10.1073/pnas.172380699.
[32] B. Adamczyk, T. Tharmalingam, P.M. Rudd, Glycans as cancer biomarkers, Biochim. Biophys. Acta - Gen. Subj. 1820 (2012) 1347–1353, https://doi.org/10.1016/j.bbagen.2011.12.001.
[33] C.I.A. Balog, K. Stavenhagen, W.L.J. Fung, C.A. Koeleman, L.A. McDonnell, A. Verhoeven, W.E. Mesker, R.A.E.M. Tollenaar, A.M. Deelder, M. Wuhrer, N-glycosylation of colorectal cancer tissues: a liquid chromatography and mass spectrometry-based investigation, Mol. Cell. Proteomics 11 (2012) 571–585, https://doi.org/10.1074/mcp.M111.011601.
[34] S.W. de Vroome, S. Holst, M.R. Girondo, Y.E.M. van der Burgt, W.E. Mesker, R.A.E.M. Tollenaar, M. Wuhrer, Serum N-glycome alterations in colorectal cancer associate with survival, Oncotarget 9 (2018) 30610–30623, https://doi.org/10.18632/oncotarget.25753.
[35] H. de Thé, Differentiation therapy revisited, Nat. Rev. Cancer 18 (2017) 117–127, https://doi.org/10.1038/nrc.2017.103.
[36] P.B. Gupta, C.L. Chaffer, R.A. Weinberg, Cancer stem cells: mirage or reality? Nat. Med. 15 (2009) 1010–1012, https://doi.org/10.1038/nm0909-1010.
[37] D. Park, K.A. Brune, A. Mitra, A.I. Marusina, E. Maverakis, C.B. Lebrilla, Characteristic changes in cell surface glycosylation accompany intestinal epithelial cell (IEC) differentiation: high mannose structures dominate the cell surface glycome of undifferentiated enterocytes, Mol. Cell. Proteomics 14 (2015) 2910–2921, https://doi.org/10.1074/mcp.M115.053983.
[38] U.K. Laemmli, Cleavage of structural proteins during the assembly of the head of bacteriophage T4, Nature. 227 (1970) 680–685.
[39] H. Towbin, T. Staehelin, J. Gordon, Electrophoretic transfer of proteins from polyacrylamide gels to nitrocellulose sheets: procedure and some applications, Biotechnology. 24 (1992) (1979) 145–149.
[40] P. Link-Lenczowski, M. Bubka, C.I.A. Balog, C.A.M. Koeleman, T.D. Butters, M. Wuhrer, A. Lityńska, The glycomic effect of N-acetylglucosaminyltransferase III overexpression in metastatic melanoma cells. GnT-III modifies highly branched N-glycans, Glycoconj. J. 35 (2018) 217–231, https://doi.org/10.1007/s10719-018-9814-y.
[41] N.H. Packer, M.A. Lawson, D.R. Jardine, J.W. Redmond, A general approach to desalting oligosaccharides released from glycoproteins, Glycoconj. J. 15 (1998) 737–747.
[42] K.R. Anumula, S.T. Dhume, High resolution and high sensitivity methods for oligosaccharide mapping and characterization by normal phase high performance liquid chromatography following derivatization with highly fluorescent anthranilic acid, Glycobiology. 8 (1998) 685–694.
[43] D.C.A. Neville, S.M. Coquard, D.A. Priestman, D.J. Te Vruchte, D.J. Sillence, R.A. Dwek, F.M. Platt, T.D. Butters, Analysis of fluorescently labeled glycosphingolipid-derived oligosaccharides following ceramide glycanase digestion and anthranilic acid labeling, Anal. Biochem. 331 (2004) 275–282.
[44] J.C. Bigge, T.P. Patel, J.A. Bruce, P.N. Goulding, S.M. Charles, R.B. Parekh, Nonselective and efficient fluorescent labeling of glycans using 2-amino benzamide and anthranilic acid, Anal. Biochem. 230 (1995) 229–238, https://doi.org/10.1006/abio.1995.1468.
[45] M.P. Campbell, L. Royle, C.M. Radcliffe, R.A. Dwek, P.M. Rudd, GlycoBase and autoGU: tools for HPLC-based glycan analysis, Bioinformatics. 24 (2008) 1214–1216, https://doi.org/10.1093/bioinformatics/btn090.
[46] J.L. Abrahams, M.P. Campbell, N.H. Packer, Building a PGC-LC-MS N-glycan retention library and elution mapping resource, Glycoconj. J. 35 (2018) 15–29, https://doi.org/10.1007/s10719-017-9793-4.
[47] M.H.J. Selman, M. Hemayatkar, A.M. Deelder, M. Wuhrer, Cotton HILIC SPE microtips for microscale purification and enrichment of glycans and glycopeptides, Anal. Chem. 83 (2011) 2492–2499, https://doi.org/10.1021/ac1027116.
[48] A.R. Hilgers, R.A. Conradi, P.S. Burton, Caco-2 cell monolayers as a model for drug transport across the intestinal mucosa, Pharm. Res. 7 (1990) 902–910 http://www.ncbi.nlm.nih.gov/pubmed/2235888 , Accessed date: 14 June 2018.
[49] L. Vila, A. García-Rodríguez, C. Cortés, R. Marcos, A. Hernández, Assessing the effects of silver nanoparticles on monolayers of differentiated Caco-2 cells, as a model of intestinal barrier, Food Chem. Toxicol. 116 (2018) 1–10, https://doi.org/10.1016/J.FCT.2018.04.008.
[50] Y. Sambuy, I. De Angelis, G. Ranaldi, M.L. Scarino, A. Stammati, F. Zucco, The Caco-2 cell line as a model of the intestinal barrier: influence of cell and culture-related factors on Caco-2 cell functional characteristics, Cell Biol. Toxicol. 21 (2005) 1–26, https://doi.org/10.1007/s10565-005-0085-6.
[51] S. Holst, A.J.M. Deuss, G.W. van Pelt, S.J. van Vliet, J.J. Garcia-Vallejo, C.A.M. Koeleman, A.M. Deelder, W.E. Mesker, R.A. Tollenaar, Y. Rombouts, M. Wuhrer, N-glycosylation profiling of colorectal cancer cell lines reveals association of fucosylation with differentiation and caudal type homebox 1 (CDX1)/villin mRNA expression, Mol. Cell. Proteomics. 15 (2016) 124–140, https://doi.org/10.1074/mcp.M115.051235.
[52] Y. Wang, D. Huang, K.-Y. Chen, M. Cui, W. Wang, X. Huang, A. Awadellah, Q. Li, A. Friedman, W.W. Xin, L. Di Martino, F. Cominelli, A. Miron, R. Chan, J.G. Fox, Y. Xu, X. Shen, M.F. Kalady, S. Markowitz, I. Maillard, J.B. Lowe, W. Xin, L. Zhou, Fucosylation deficiency in mice leads to colitis and adenocarcinoma, Gastroenterology 152 (2017) 193–205 (e10), https://doi.org/10.1053/j.gastro.2016.09.004.
[53] J.M. Pickard, A.V. Chervonsky, Intestinal fucose as a mediator of host-microbe symbiosis, J. Immunol. 194 (2015) 5588–5593, https://doi.org/10.4049/jimmunol.1500395.
[54] J.M. Pickard, C.F. Maurice, M.A. Kinnebrew, M.C. Abt, D. Schenten, T.V. Golovkina, S.R. Bogatyrev, R.F. Ismagilov, E.G. Pamer, P.J. Turnbaugh, A.V. Chervonsky, Rapid fucosylation of intestinal epithelium sustains host-commensal symbiosis in sickness, Nature 514 (2014) 638–641, https://doi.org/10.1038/nature13823.
[55] S.S. Pinho, P. Oliveira, J. Cabral, S. Carvalho, D. Huntsman, F. Gärtner, R. Seruca, C.A. Reis, C. Oliveira, Loss and recovery of Mgat3 and GnT-III mediated E-cadherin N-glycosylation is a mechanism involved in epithelial-mesenchymal-epithelial transitions, PLoS One 7 (2012) e33191, , https://doi.org/10.1371/journal.pone.0033191.
[56] N. Choudhry, M. Bajaj-Elliott, V. McDonald, The terminal sialic acid of glycoconjugates on the surface of intestinal epithelial cells activates excystation of Cryptosporidium parvum, Infect. Immun. 76 (2008) 3735–3741, https://doi.org/10.1128/IAI.00362-08.
[57] S. Sakarya, C. Göktürk, T. Öztürk, M.B. Ertugrul, Sialic acid is required for non-specific adherence of *Salmonella enterica ssp. enterica* serovar Typhi on Caco-2 cells, FEMS Immunol. Med. Microbiol. 58 (2010) 330–335, https://doi.org/10.1111/j.1574-695X.2010.00650.x.
[58] N.D. McDonald, J.-B. Lubin, N. Chowdhury, E.F. Boyd, Host-derived sialic acids are an important nutrient source required for optimal bacterial fitness in vivo, MBio. 7 (2016) e02237-15, , https://doi.org/10.1128/mBio.02237-15.
[59] T. Haselhorst, F.E. Fleming, J.C. Dyason, R.D. Hartnell, X. Yu, G. Holloway, K. Santegoets, M.J. Kiefel, H. Blanchard, B.S. Coulson, M. von Itzstein, Sialic acid dependence in rotavirus host cell invasion, Nat. Chem. Biol. 5 (2009) 91–93, https://doi.org/10.1038/nchembio.134.
[60] D. Zalem, J.P. Ribeiro, A. Varrot, M. Lebens, A. Imberty, S. Teneberg, Biochemical and structural characterization of the novel sialic acid-binding site of Escherichia coli heat-labile enterotoxin LT-IIb, Biochem. J. 473 (2016) 3923–3936, https://doi.org/10.1042/BCJ20160575.
[61] H.J. An, P. Gip, J. Kim, S. Wu, K.W. Park, C.T. McVaugh, D.V. Schaffer, C.R. Bertozzi, C.B. Lebrilla, Extensive determination of glycan heterogeneity reveals an unusual abundance of high mannose glycans in enriched plasma membranes of human embryonic stem cells, Mol. Cell. Proteomics 11 (2012), https://doi.org/10.1074/mcp.M111.010660 (M111.010660).
[62] K. Hasehira, H. Tateno, Y. Onuma, Y. Ito, M. Asashima, J. Hirabayashi, Structural and quantitative evidence for dynamic glycome shift on production of induced pluripotent stem cells, Mol. Cell. Proteomics 11 (2012) 1913–1923, https://doi.org/10.1074/mcp.M112.020586.